American Mineralogist, Volume 83, pages 1067–1076, 1998

Sulfur and iron surface states on fractured pyrite surfaces

H.W. Nesbitt,[1,*] G.M. Bancroft,[2] A.R. Pratt,[2] and M.J. Scaini[2]

[1]Department of Earth Sciences, University of Western Ontario, London, Ontario N6A 5B7, Canada
[2]Department of Chemistry, University of Western Ontario, London, Ontario N6A 5B7, Canada

Abstract

Pyrite has a poor {001} cleavage. Unlike most other minerals with a rocksalt-type structure, pyrite typically fractures conchoidally, demonstrating that parting surfaces are not constrained to the {001} crystallographic plane. Cleavage along {001} require rupture of only Fe-S bonds, but pyrite consists of both Fe-S and S-S bonds. Analysis of bond energies indicates that S-S bonds are the weaker bonds and they are likely to be ruptured when pyrite is fractured. With each ruptured S-S bond, two mononuclear species (formally S^{1-}) are produced, one bound to one fracture surface and the second to the opposite fracture surface. This monomer is reduced to S^{2-} (monosulfide) during relaxation through oxidation of surface Fe^{2+} ions to Fe^{3+}. These surface relaxation processes explain the surface states observed in S(2p) and Fe($2p_{3/2}$) X-ray photoelectron spectra (XPS) of pyrite. The S(2p) XPS spectrum is interpreted to include bulk disulfide contributions at 162.6 eV and two surface state contributions at 162.0 and 161.3 eV. The monosulfide (S^{2-}) emission is near 161.3 eV, as observed in S(2p) spectra of pyrrhotite, and the 162 eV peak is interpreted to result from the surface-most sulfur atom of surface disulfide ions. The Fe($2p_{3/2}$) XPS spectrum includes three contributions, a bulk Fe^{2+} emission near 707 eV and emissions from two Fe surface states. One surface state is interpreted to be Fe^{2+} surface ions. Their coordination is changed from octahedral before fracture to square pyramidal after fracture. The consequent stabilization of the antibonding Fe d_{z^2} orbital yields unpaired electrons in the valence band resulting in multiplet peak structure in the Fe($2p_{3/2}$) spectrum. Similarly, each surface Fe^{3+} ion, having contributed a non-bonding 3d electron to the valence band (bonding orbital), contains unpaired 3d electrons, resulting in multiplet splitting of its Fe($2p_{3/2}$) signal. The high-energy tail observed in the Fe($2p_{3/2}$) spectrum of pyrite is the product of emissions from both surface states with Fe^{2+} multiplet peaks centered near 708 eV and the surface Fe^{3+} multiplets spanning the binding energies from 708.75 to about 712 eV.

Introduction

Mineral fracture surfaces are commonly exposed to natural solutions in sedimentary environments and during mining operations. Transport of sediment within fluvial and coastal marine sedimentary environments results in innumerable grain-grain collisions, and production of fracture surfaces through abrasion. Similarly, glaciation exposes fresh fracture surfaces to natural weathering solutions. Much of the Northern Hemisphere now is blanketed in glacially derived detritus. From an industrial perspective, fresh fracture surfaces are produced by milling in preparation for flotation. Pyrite is the most common of sulfide minerals, and the chemical state of its fracture surfaces is the focus of this study.

Fractured pyrite surfaces react with aerated solutions of sedimentary environments, generally to produce Fe-oxyhydroxides and sulphuric acid. Pyrite is an abundant mineral in mine wastes where it again reacts with aerated solutions to produce high concentrations of sulphuric acid observed in acidic mine waste waters. The chemical states of pyrite and other sulfide mineral fracture surfaces are vitally important to efficient separation of ore minerals from gangue (e.g., pyrite) during flotation. A complete understanding of natural weathering processes, mineral processing, and treatment of mine wastes necessarily begins with documentation of pristine fracture surfaces, thus motivating detailed study of such surfaces.

Recent interest in the nature of sulfur species at pristine pyrite surfaces is substantial. Hyland and Bancroft (1989) and Nesbitt and Muir (1994) noted a major disulfide contribution to the S(2p) X-ray photoelectron spectra (XPS) spectrum of a fractured, unreacted pyrite surface, but required a small contribution to both the low and high energy sides of the disulfide peak to properly fit the spectrum. Bronold et al. (1994) recognized a distinct peak on the low energy side of the disulfide peak and ascribed it to a surface disulfide species. Termes et al. (1987) and Buckley et al. (1988) documented the S(2p) spectrum of

* E-mail: hwn@julian.uwo.ca

0003–004X/98/0910–1067$05.00

transition metal polysufides and established that polysulfide binding energies are at slightly higher binding energy than the disulfide peak, and intermediate between disulfide and elemental sulfur (end-members of the polysulfide series). Mycroft et al. (1990) observed abundant polysulfide species on reacted pyrite surfaces by both in-situ Raman and XPS techniques. Their polysulfide contribution was observed on the high energy side of the disulfide peak, and within the range of binding energies established by Termes et al. (1987) and Buckley et al. (1988). On this basis, Nesbitt and Muir (1994) assigned the high-binding energy peak to polysulfide and interpreted the S(2p) spectrum to include 85% disulfide (S_2^{2-}), about 10% S^{2-} (monosulfide) and approximately 5% polysulfide (S_n^{2-}). An interpretation of the S(2p) XPS spectrum is here offered, which resolves previous differences in interpretation and provides an explanation for unusual features of the pyrite Fe($2p_{3/2}$) spectrum.

The Fe($2p_{3/2}$) spectrum of pyrite contains a strong, near-symmetrical peak in the region of 707 eV, but also contains a weak but distinct high-energy tail that extends to about 712 eV. Numerous explanations for the tail have been offered (Nesbitt and Muir 1994), but none are completely satisfactory. The electronic configuration of bulk and surface Fe^{2+} ions is considered here with emphasis placed on electronic states in the valence band. Fe^{2+} of bulk pyrite exists as a low-spin state, but ligand field considerations indicate that surface Fe ions have unpaired electrons in the valence band. These unpaired electrons can result in multiplet splitting of the Fe($2p_{3/2}$) spectral peaks, and this aspect receives detailed consideration.

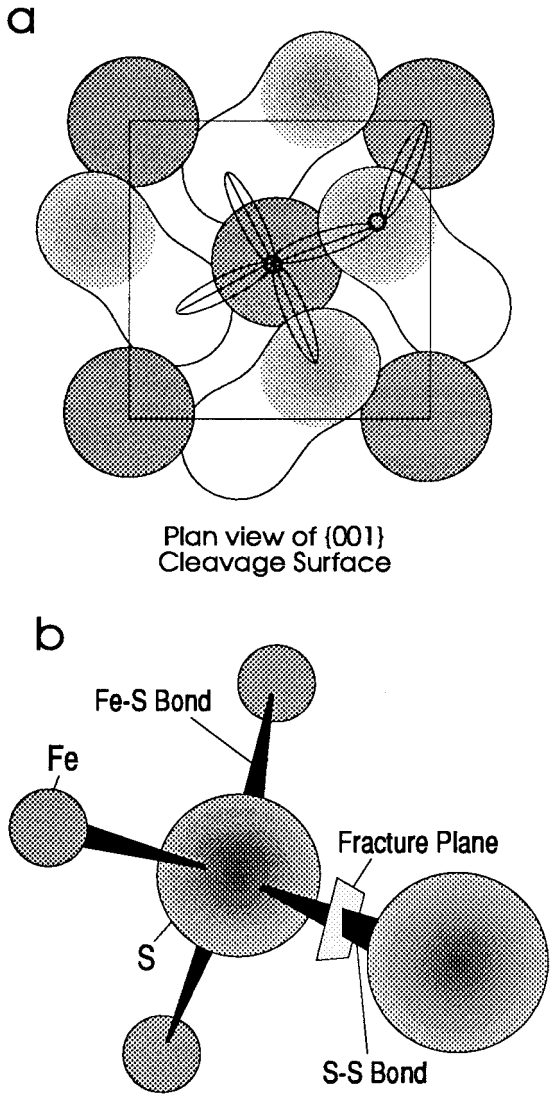

Figure 1. (**a**) Fe and S_2^{2-} ions at the pyrite {001} surface. The Fe ions are represented by shaded circles and the dianion by elongate ''dumbbells''. The shaded end of the dumbbells extends slightly above the plane containing the face-centered and corner-shared cations, and the other end of the dumbbells are below the plane. The square outlines the unit cell. The ellipses, with long axis shown, illustrate Fe-S bonds. The face-centered Fe ion is bonded to a disulfide beneath the plane shown, and to another disulfide above the plane drawn to achieve octahedral coordination. S-S bonds are not shown but extend from the center of the shaded end to the center of the other end. (**b**) A portion of the Fe-S_2 cluster in pyrite, and the configuration of Fe-S and S-S bonds. One S atom of the dianion is shown bonded to three Fe ions. The second S atom is similarly bonded to three Fe ions but to preserve clarity these are not shown.

Properties of pyrite

Structure and bonding

Pyrite can be considered a derivative of the rocksalt structure with lower symmetry (*Pa*3) because the dianion S_2^{2-} is elongate (dumbbell shaped). Its long axis is ''tilted'' relative to the crystallographic axes, and resides in two (opposed) orientations in the pyrite unit cell, thus lowering its symmetry (Fig. 1a). Minerals with rocksalt-like structures commonly have perfect {001} cleavage, primarily because a minimum number of cation-anion bonds have to be broken in this plane, and because this cleavage surface is autocompensated and displays a substantially lower surface energy than other surfaces such as {110} or {111} (Henrich and Cox 1994). Pyrite, in contrast, displays poor {001} cleavage (Deer et al. 1992) and commonly a conchoidal fracture (Eggleston et al. 1996). It differs in another respect; there is one type of bond in halite, the Na-Cl bond, but two in pyrite, Fe-S and S-S bonds (Figs. 1b, 2a and 2b).

XPS S(2p) and Fe($2p_{3/2}$) spectra

Numerous studies have reported the XPS S(2p) spectral properties of pyrite parting surfaces. Nesbitt and Muir (1994) observed a sulfur surface state in the XPS S(2p) spectrum with a binding energy similar to the monosulfide anion (S^{2-}) of pyrrhotite. Bronold et al. (1994) conducted a synchrotron experiment in which S(2p) XPS spectra were collected at different photon energies. They obtained unequivocal evidence for two sulfur surface states at 161.3 and 162.0 eV (Fig. 2) that are 0.6 and 1.3 eV lower than the bulk disulfide binding energy (162.6

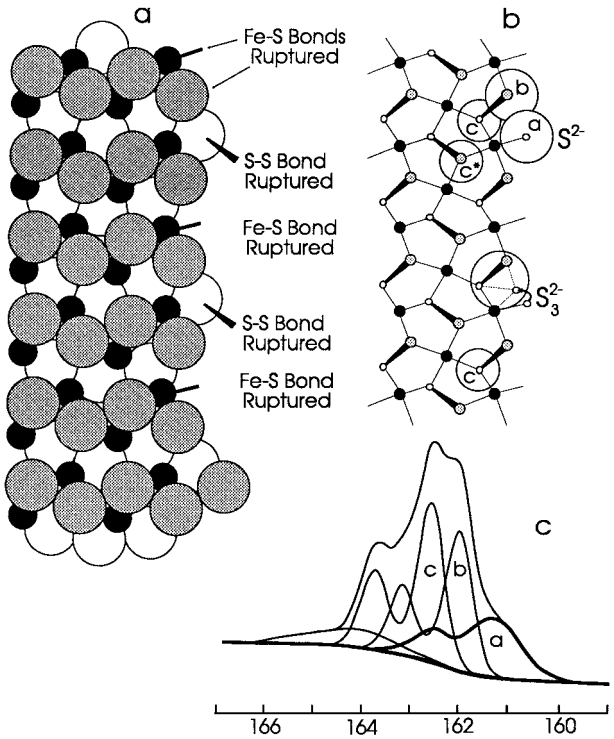

FIGURE 2. Structural and bonding relations in the near-surface region of a pyrite fracture surface, and a XPS S(2p) spectrum of a fractured pyrite surface (modified after Bronold et al. (1994). (**a**) Arrangements of S and Fe ions exposed on an atomically rough surface approximately parallel to the {001} plane. Black dots = Fe^{2+} ions. Shaded circles = S atoms of disulfide situated in a plane immediately ''above'' the plane containing the Fe ions. Large open circles = S atoms of disulfide located in a plane beneath the plane containing the Fe ions. (**b**) A ball and stick equivalent of (a). Dots = Fe^{2+} ions Disulfide, pairs of patterned and open circles connected by a wedge-shaped line. Patterned circles are situated ''above'' the Fe plane, and open circles below it. The thick end of the connecting line indicates the ''tilt'' on the disulfide. Thin straight lines represent Fe-S bonds. The large circle labeled ''a'' represents the surface states of monosulfide; (''b''), the surface-most S atom of the surface disulfide; (''c''), fully coordinated near-surface S atoms of disulfides; and ''c*'' S atoms of bulk disulfide. A polysulfide surface state (S_n^{2-}) is also noted. (**c**) An S(2p) XPS spectrum of a fractured pyrite surface at the bottom of the diagram illustrates the various contributions to the spectrum by the letters, which correspond to the various surface and bulk states of the above ball-and-stick diagram.

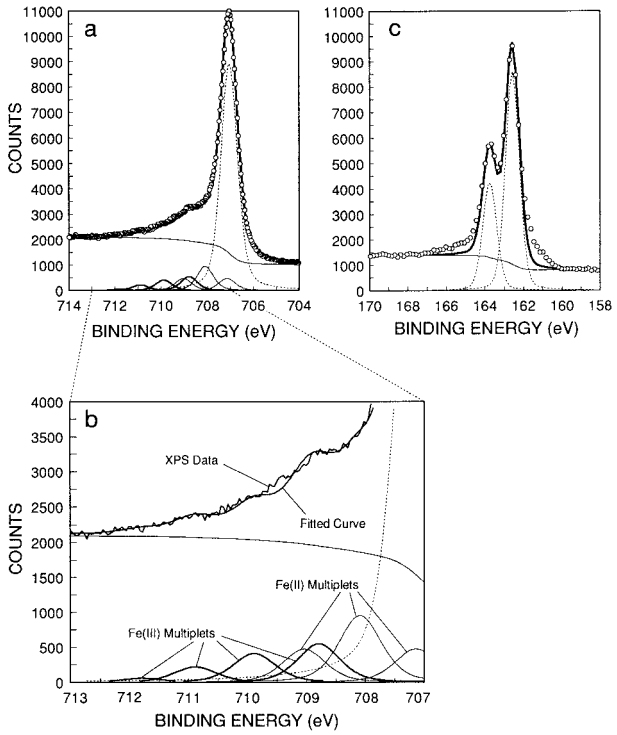

FIGURE 3. High resolution Fe($2p_{3/2}$) (**a**) and S(2p) (**c**) spectra of vacuum-fractured pyrite. (**b**) is an expansion of the high-energy tail. Spectrometer settings were 50 eV pass energy and 300 μm X-ray spot size for collection of the spectra. Other instrumental settings and conditions are provided by Splinter et al. (1997). Circles = experimental data. Thick solid curves = the fit to each spectrum. The disulfide doublet is separated by 1.18 eV and both have the same FWHM. The light solid line is the Shirley background.

eV). These large binding energy shifts are unexpected for an autocompensated surface, and indicate that the surface states differ substantially from the bulk disulfide.

The XPS Fe($2p_{3/2}$) spectrum of pyrite has a major peak near 707 eV and an unusual, low intensity, wedge-shaped tail on the high energy side of the main peak (Fig. 3a). It has no peak maximum hence is uncharacteristic of a shakeup or other satellite peak. Neither can it be easily explained as a ''metal-like'' tail (Doniach and Sunjic 1970) because its shape differs from that of Fe metal peaks (Nesbitt and Muir 1994). As pyrite remained a semiconductor in this study and in all XPS studies reported here, the tail cannot be explained by the Doniach-Sunjic ''process'' (the conduction band of pure pyrite is empty, but it may be somewhat populated if dopant levels are significant). The wedge-shaped tail of the Fe(2p) spectrum may result from photoelectron emissions from Fe surface states and this possibility is investigated.

Pyrite {001} cleavage surface

Based solely on structure and number of bonds ruptured, the {001} cleavage of pyrite should be near-perfect, as it is for halite. Planes parallel to the {001} surface of pyrite (and equidistant from face-centered Fe ions) intersect only Fe-S bonds and their cleavage produces the ''rocksalt cleavage surface'' shown in Figure 1a. This surface is autocompensated as shown by the following calculation. Using the formalism of Gibson and LaFemina (1996) and Harrison (1980), we begin with neutral Fe and S atoms (the same conclusions are reached if one begins with Fe^{2+} and S_2^{2-} ions). Each Fe atom would have two valence electrons available to contribute to creation of each of the six Fe-S bonds, thus contributing a third of

an electron for each bond to be formed. Two sulfur atoms have six valence electrons each, for a total of twelve. Each sulfur atom is tetrahedrally coordinated in pyrite, three apices directed toward Fe atoms and the fourth toward the second sulfur atom. Two of the twelve valence electrons are consequently shared by the two sulfur atoms to form the S-S bond (and S_2 dimers). The remaining ten are available to be shared among the six equidistant Fe atoms, thus there are $\frac{5}{3}$ electrons from S_2 available for creation of each Fe-S bond. The same electronic contributions are available from each Fe atom and S_2 dimer located at pyrite cleavage surfaces. Some contributions, however, would be to the dangling bonds extending from the surface, and surface relaxation likely would involve transfer of electrons from some dangling bonds to others in an attempt to achieve a more stable surface. Specifically, the ⅓ electrons of dangling bonds associated with surface Fe atoms may be transferred to dangling bonds of surface S_2 dimers containing $\frac{5}{3}$ electrons per dangling bond. The results are completely empty cation dangling bonds, and completely filled anion dangling bonds (two electrons per bonding orbital). Such a transfer produces electronically stable cation and anion surface states, which stabilizes the entire surface. The surface is stable and charge neutral, therefore autocompensated (Gibson and LaFemina 1996).

However, pyrite displays irregular fracture surfaces that are obviously not restricted to {001}, or any other crystallographic plane. Pyrite contains cation-anion bonds (Fe^{2+}-S_2^{2-} bond is equivalent to the Na-Cl bond) as well as S-S bonds (no equivalent in halite). The presence of the S-S bond may have a substantial affect on cleavage properties if the energy required to rupture it is less than the energy needed to rupture the Fe^{2+}-S_2^{2-} bond. Fe-Cl, Fe-Br, and Fe-I bond energies in $FeCl_2$, $FeBr_2$, and FeI_2 are respectively 400, 340, and 280 kJ/mol (Huheey 1978, Appendix F). The ionic radii of the iodide and disulfide anions are almost identical (2.06 and 2.08 Å, respectively). The disulfide is, however, doubly charged so that the Fe^{2+}-S_2^{2-} bond energy should be approximately twice that of the Fe-I bond according to the Born-Mayer equation. The Fe^{2+}-S_2^{2-} bond energy is clearly greater than 300 kJ/mol and is likely to be appreciably greater than 400 kJ/mol. The S-S bond energy is lower, 245 ± 20 kJ/mol (Huheey 1978, Appendix F), suggesting that the weaker S-S bond should be ruptured during fracture. Although production of irregular fracture surfaces requires rupture of more bonds than does production of the {001} cleavage surface, the energy saved by breaking S-S bonds (rather than Fe^{2+}-S_2^{2-} bonds) could compensate for the greater number of bonds broken.

The above bond energy considerations strongly suggest that a realistic understanding of pyrite surface properties must include consideration of irregular surfaces. Many of these surfaces will be polar, non-autocompensated, unstable, and likely to have associated, reactive surface states.

Pyrite fracture surfaces

Although planes parallel to {001} intersect only Fe-S bonds, most other planes intersect both Fe-S and S-S bonds. Where an S-S bond is intersected (Fig. 1b), the bond will remain intact only if three Fe-S bonds at either end of the dianion are broken instead of the S-S bond. The energetics of such are not favorable. The consequence is that S-S bonds are likely to be ruptured during fracture of pyrite, producing unique surface sulfur states.

Rupture of an S-S bond leaves one sulfur monomer (nominally S^-) on one fracture surface and the other on the opposite surface. Their presence leads to a high probability of producing ''local,'' noncompensated, and thermodynamically unstable regions surrounding the S monomer. Using the formalism of Gibson and LaFemina (1996), ⅓ of an electron is associated with each dangling bond of surface Fe atoms. If a surface sulfur monomer were produced upon fracture (an S-S bond severed), there would be six electrons available to contribute to four bonds (one a dangling bond), averaging 1.5 electrons per bond. Transfer of the ⅓ electron to the surface S^- dangling bond would yield 11/6 electrons per dangling bond on the sulfur monomer, a value short of the two electrons per bonding orbital needed to stabilize the surface state and to achieve charge neutrality (to be autocompensated). Autocompensation around the sulfur monomer can be attained by oxidizing Fe^{2+} to Fe^{3+} and reducing the S^{1-} monomer to S^{2-}, as now discussed.

Surface relaxation and surface states

Relaxation

Sulfur monomers with a formal valence of 1− (S^{1-}) represent an enigmatic aspect associated with relaxation of pyrite fracture surfaces. Mineralogical studies indicate S^{2-} and disulfide (S_{2-}^2) are commonly present in naturally occurring sulfide minerals (Pratt et al. 1994; Buckley and Woods 1985). Transition metal polysulfides (S_n^{2-}, $2 < n < 8$) are also well established (Termes et al. 1987; Buckley et al. 1988). Although many states of sulfur, including elemental sulfur (S_8^0), have been reported for minerals, S^{1-} has not been observed in nature. If produced at pyrite fracture surfaces, it may undergo significant modification during relaxation.

Modification to bond angles or lengths, or migration of species to or from the surface does little to address the formal oxidation state of the S^{1-} monomer. The simplest and perhaps the most reasonable means to stabilize the monomer is to fill the 3p orbitals to attain a filled octet, hence a stable ''Ar'' configuration. In effect, the unstable S^{1-} monomer may ''relax'' to the more stable monosulfide (S^{2-}) found in minerals such as pyrrhotite. The S^{2-} surface species may acquire the additional electron from adjacent Fe^{2+} ions to produce, in effect, surface Fe^{3+} and S^{2-} ions:

$$Fe^{2+}_{surface} + S^{-}_{surface} \rightarrow Fe^{3+}_{surface} + S^{2-}_{surface}. \quad (1)$$

From a band theory perspective, an unoccupied S sur-

face electronic state is produced by fracture, but is subsequently filled during relaxation by acquisition of an Fe(3d) electron (top-of-valence band is depleted). The mechanism for transfer is uncertain, but Goodenough (1982) shows that there can be strong overlap of the Fe(3d) density of states with the S(2p) density of states thus allowing electron transfer to the anion with minimal energy input. As well, the energy associated with fracturing may promote temporarily an Fe(3d) electron to the conduction band where it migrates to, and becomes localized on, a S^{1-} site to produce S^{2-}. Reaction 1 is consistent with the principles governing surface relaxation (Gibson and LaFemina 1996) where electrons of antibonding metal orbitals are transferred to adjacent anions to fill their bonding orbitals. The transfer leads to an autocompensated region surrounding the S^{2-} and Fe^{3+} surface states, as noted previously.

The second possibility for production of S^{2-} surface states is acquisition of electrons from other S^{1-} monomers. Electrons from some S^{1-} sites may become delocalized, perhaps promoted to the conduction band by energy derived from fracturing the mineral. Once delocalized they migrate to other S^{1-} sites where they again become localized to produce stable S^{2-} (filled octet). This ''disproportionation'' results in production of S^0 and S^{2-} monomers at the surface and may be represented formally by:

$$2S^{1-}_{surface} \rightarrow S^{0}_{surface} + S^{2-}_{surface}. \quad (2)$$

The S^0 species may remain a monomer or may react with a subtending disulfide to produce polysulfide (S_3^{2-}) in the near-surface as shown in Figure 2b.

Evidence from arsenopyrite surfaces

Arsenic in arsenopyrite is bonded to S to yield an As-S dianion akin to disulfide of pyrite. The formal charge on each of As and S is 1− (as for pyrite). XPS study of pristine arsenopyrite surface (Nesbitt et al. 1995) demonstrates that about 85% of As is present as the dimer (As-S) and about 15% as As^0. About 15% of sulfur is present as S^{2-} (monosulfide) thus allowing for charge neutrality (Nesbitt et al. 1995). Production of a parting surface may cause surface As-S bonds to be severed. Relaxation then occurs with electrons being localized preferentially on the more electronegative S atom rather than on the As atom. The consequence is production of S^{2-} and As^0 at arsenopyrite fracture surfaces. The reaction may be represented by:

$$As\text{-}S_{surface} \rightarrow As^{0}_{surface} + S^{2-}_{surface}. \quad (3)$$

The XPS spectra of Nesbitt et al. (1995) provide evidence for the production of surface monosulfide (S^{2-}) at fractured arsenopyrite surfaces, and considering the similarities between pyrite and arsenopyrite, the data provide circumstantial support for the presence of S^{2-} at fractured pyrite surfaces.

S(2p) and Fe($2p_{3/2}$) XPS spectra reinterpreted

S(2p) spectrum

Bulk states. By decreasing the photon excitation energy, thus increasing surface sensitivity, Bronold et al. (1994) demonstrated that the peak at 162.6 eV represented a bulk emission (Fig. 2c). The peaks at 162.0 and 161.3 eV became more intense as surface sensitivity increased, demonstrating that these two peaks represented surface states. Bronold et al. (1994) based their interpretation of sulfur surface states on a perfect {001} cleavage surface, that is only Fe-S bonds were considered to have been severed during fracture, leaving all S-S bonds intact. They consequently considered disulfide (S_2^{2-}) to be the only anionic species present on pyrite fracture surfaces, and sulfur surface states were interpreted to arise solely from disulfide. As did Bronold et al. (1994), we interpret the peak at 162.6 eV (Fig. 2c) to represent emissions from S atoms of bulk disulfide (e.g., states c, c*, and deeper S atoms of Fig. 2b).

S_2^{2-} and S_{2-} surface states. The pyrite fracture surface of Figure 2 shows the effects of ruptured Fe-S and S-S bonds, and the consequent presence of surface disulfide (S_2^{2-}) and monosulfide (S^{2-}) ions (Figs. 2a and 2b). The surface-most disulfide ion contains S atoms labeled ''b'' and ''c'' (Fig. 2b). The atom labeled ''b'' is not fully coordinated because at least one Fe-S bond has been severed with the Fe ion residing on the opposite face. The S atom labeled ''c'' is fully coordinated (fourfold). The surface-most atom ''b'' is more likely to produce a surface state (low coordination). Bronold et al. (1994) appealed to an electric ''double layer'' within the near-surface to argue that atom ''b'' contributed to the peak at 161.3 eV and assigned the emission from atom ''c'' to the peak at 162.0 eV. These assignments would, however, yield a peak at 161.3 eV that was more intense than the peak at 162.0 eV (considering attenuation), contrary to observation (Fig. 2c). To address the inconsistency, Bronold et al. (1994) assigned the S atom labeled ''c*'' (Fig. 2b) to the peak at 162.0 eV (Fig. 2c). This partially overcomes the intensity problem but produces another. The S atoms ''c'' and ''c*'' are located at different positions within the electric ''double layer'', and should give rise to a different binding energy shift for each type of atom. If, as proposed by Bronold et al. (1994), the peak at 162.0 eV includes contributions from S atoms ''c'' and ''c*'', the peak should be broad because the two contributions have different binding energies. The peak is, however, narrow and provides no indication of being a composite. Assignment of the ''c*'' emission to the 162.0 eV peak is therefore questioned. This atom is located at the extreme lower boundary of the electric double layer and is fully coordinated, hence is likely to be bulk-like and contribute to the 162.6 eV bulk peak rather than the surface state peak at 162.0 eV.

Although the electric ''double layer'' should cause shifts in binding energy of near-surface S atoms, this effect may not be the only contribution to such shifts. Spe-

cifically, binding energy shifts resulting from S atoms of different coordination number have not been included in the considerations of Bronold et al. (1994), although coordination is known to affect binding sulfur energies. S atoms in CuS and pentlandite, for example, display two coordinations. In both minerals, S of low coordination has somewhat lower binding energies than the more highly coordinated S atoms (Legrand et al. 1998; Laajalehto et al. 1996). S atoms at pyrite fracture surfaces are necessarily of lower coordination (due to bond scission) than bulk S atoms, and a peak shift to lower binding energy is expected, just as observed for low coordinate S atoms in these minerals. A simple interpretation of the S(2p) surface states is presented that focuses on the chemical state of S atoms.

Monosulfide (Fig. 2b, state ''a'') is produced by rupture of a S-S bond but it necessarily remains bonded to Fe. After relaxation to S^{2-} it should have spectral properties akin to S^{2-} of pyrrhotite. The monosulfide (S^{2-}) peak of pyrrhotite is situated at 161.25 ($\pm$0.1) eV (Pratt et al. 1994; Buckley and Woods 1985), and the pyrite S(2p) surface state at 161.3 eV (Fig. 2c) is consequently interpreted to represent a S^{2-} surface state (Figs. 2b and 2c, ''a''). The monosulfide (Fig. 2b, state ''a'') alone is considered to contribute to the peak at 161.3 eV. The low-coordinate S atom ''b'' of the surface disulfide ion (Fig. 2b) is assigned to the peak at 162.0 eV, whereas the fully coordinated S atoms ''c'', ''c*'', and all S atoms deeper than these are assigned to the bulk contribution at 162.6 eV. By this interpretation, the relative intensity of the surface state peaks (161.3 and 162.0 eV) is a direct measure of the number of S-S and Fe-S bonds broken during fracture.

A second interpretation combines elements of the Bronold proposals and ours. Sulfur atoms ''a'' and ''b'' contribute to the 161.3 eV peak, ''c'' and ''c*'' contribute to the peak at 162.0 eV, and all deeper atoms contribute to the bulk peak at 162.6 eV. The ambiguities associated with this interpretation already have been discussed. It assumes that ''c'' and ''c*'' yield photoemissions of identical binding energy although they are located at different depths from the surface. It also assumes that S atoms of substantially different chemical state give rise to surface states of similar binding energies. Most striking is that the same binding energy must be assigned to the monosulfide (S^{2-}) and the ''b'' atom of the surface disulfide ion. Their chemical states are much different and the assignment seems unlikely.

S_n^{2-} surface states. An additional surface state, S_3^{2-}, is shown in Figure 2b. Although its existence is not certain, the state may arise from rupture of an S-S bond, with subsequent transfer of an electron to another S monomer as discussed previously (reaction 2). The resulting ''S^0'' species may react with the immediately underling disulfide to produce polysulfide (S_3^{2-}) by analogy with reactions in aqueous solutions; little energy is required to produce S_3^{2-} from S^0 (solid) and aqueous disulfide (Langmuir 1997; Johnson 1982). The abundance of polysulfides on leached pyrite surfaces attests to the viability of the reaction (Mycroft et al. 1990). Binding energies of polysulfide range between about 162.5 eV (disulfide) and 164.0 eV (elemental sulfur), hence its detection in the S(2p) XPS spectrum is difficult due to the large number of spectral contributions to this region (Fig. 2c).

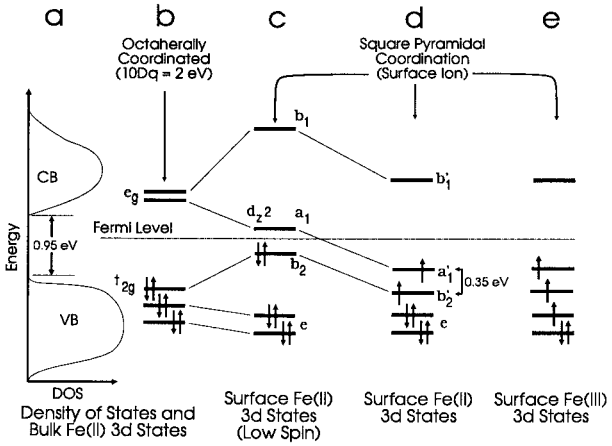

FIGURE 4. The Fe(3d) ligand field splitting due to reduced coordination resulting from fracture. Fe^{2+} is octahedrally coordinated before fracture and square pyramidal after fracture. (**a**) represents the bulk density of states (DOS) for pyrite, (**b**) the electronic levels for Fe^{2+} in bulk pyrite in octahedral coordination, (**c**) electronic levels of surface Fe^{2+} in square pyramidal coordination (low-spin state), (**d**) electronic levels of surface Fe^{2+} in square pyramidal coordination with one unpaired electron in the d_{z^2} level, and (**e**) electronic levels of surface Fe^{3+} in square pyramidal coordination with one unpaired electron in the d_{z^2} level. The ordinate is not drawn to scale. CB denotes conduction band and VB denotes the valence band. Primes indicate unpaired electrons. The energy separating a_1 and b_2 in (**c**) and (**d**) is 0.35 eV and the electron pairing energy is about 1.6 eV for square pyramidal symmetry. The diagram is modified after that of Bronold et al. (1994, Fig. 2).

Fe($2p_{3/2}$) spectrum

Production of S^{2-} surface states on pyrite through oxidation of Fe^{2+} should produce an Fe^{3+} surface state, the surface concentration of which will be the same as S^{2-} provided all S^{2-} is formed by the process represented by reaction 1. Detection of the monosulfide (S^{2-}) in the S(2p) spectrum consequently suggests that the ferric state should be detectable in the Fe(2p) spectrum, and indeed the main peak of the Fe($2p_{3/2}$) spectrum (Fig. 4) has a high-energy tail that is not expected if only Fe^{2+} bonded to disulfide were present in the near-surface. An explanation is pursued by first evaluating likely electronic states of Fe at pyrite surfaces.

Fe^{2+}(3d) states. The molecular orbital and consequent band models of Bronold et al. (1994) are summarized in Figure 4. The density of states (DOS) diagram for bulk pyrite is shown in Figure 4a. The energy axis is not drawn to scale. The valence band includes Fe-S_2 and S-S σ-bonds. The three Fe(3d) t_{2g} non-bonding orbitals are lo-

cated at the top of the valence band and extend to just below the Fermi level. Antibonding 3p, 4p, 4s, and the two e_g 3d orbitals of Fe, and antibonding sp^3 orbitals of sulfur (Bronold et al. 1994) all contribute to the conduction band (CB). The two bulk Fe^{2+} e_g orbitals are sufficiently destabilized by the six surrounding dianions that all electrons are paired and reside in the non-bonding t_{2g} orbitals yielding a low-spin configuration (Fig. 4b). A consequence is that bulk Fe^{2+} will be represented by a single peak in the Fe($2p_{3/2}$) spectrum; multiplet splitting should not occur because unpaired electrons do not exist in the valence band of bulk Fe^{2+}.

The analysis of Bronold et al. (1994) indicates that the t_{2g} and e_g orbitals are non-bonding and antibonding, respectively, and hence may be treated by ligand field theory to a first approximation. Upon fracture, the octahedral coordination of surface Fe becomes square planar-pyramidal (C_4V point group) due to loss of one dianion. This results in stabilization of the d_{z_2} orbital (Fig. 4c, a_1 level) and slight destabilization of the d_{xy} orbital (Fig. 4c, b_2 level) so that there is only 0.35 eV separating the two levels (Fig. 4c). The electron pairing energy is sufficiently large (about 1.6 eV for C_4V symmetry, Bronold et al. 1994) that the energy of an unpaired electron in the d_{z_2} orbital is located below the Fermi level and within the valence band (Fig. 4d, a_1' level). The large pairing energy and the small energy difference between a_1 and b_2 levels favor promotion of an electron from the t_{2g} orbital into the a_1' (e_g) orbital (Figs. 4c and 4d) to yield an intermediate spin state for Fe^{2+} surface ions (Fig. 4d). Surface Fe^{2+} ions accordingly have unpaired electrons in the valence band, leading to multiplet splitting of their XPS(2p) signal.

The high-spin state multiplet structure for Fe^{2+} ion has been evaluated (Gupta and Sen 1974, 1975), but the multiplet structures for intermediate spin states are unknown. If the Fe^{2+}, Mn^{4+}, and Cr^{3+} high-spin states can be used as guides, then the $2p_{3/2}$ XPS spectrum of Fe^{2+} in intermediate spin state includes three or four multiplet peaks, each separated by about 1 eV (Gupta and Sen 1975; McIntyre and Zetaruk 1977; Pratt and McIntyre 1996). The Fe^{2+} high-spin multiplet structure includes three peaks with each separated by about 1 eV in pyrrhotite (Pratt et al. 1994), magnetite (McIntyre and Zetaruk 1977) and for the free ion (Gupta and Sen 1975). It is used subsequently as a guide to fit the Fe^{2+} surface contribution to the Fe($2p_{3/2}$) spectrum (Figs. 3a and 3b) solely because it meets the general criteria just stated. This is not to suggest that Fe^{2+} of intermediate and high-spin states have the same multiplet structure.

Fe^{3+}(3d) states. If monosulfide (S^{2-}) develops on fractured pyrite surfaces through oxidation of a surface Fe^{2+} ion, then surface Fe^{3+} ions should represent a third contribution to the Fe($2p_{3/2}$) spectrum. The electron removed from surface Fe^{2+} can be derived either from the a_1 or e level (Figs. 4d and 4e), depending on the pairing energy and the energy difference between the a_1 and e levels. At least one unpaired Fe^{3+} electron is present in the valence band so that surface Fe^{3+} ions should display multiplet peaks in the Fe($2p_{3/2}$) XPS spectrum. As are surface Fe^{2+} ions, surface Fe^{3+} ions are in an intermediate spin state, the multiplet structure of which is unknown. If Fe^{3+} and Cr^{4+} high-spin states can be used as guides, then the $2p_{3/2}$ XPS structure of Fe^{3+} in intermediate spin state includes three or four multiplet peaks, each separated by about 1 eV (Gupta and Sen 1975; McIntyre and Zetaruk 1977; Pratt and McIntyre 1996). The Fe^{3+} high-spin multiplet structure includes four peaks with each separated by about 1 eV (Gupta and Sen 1975; McIntyre and Zetaruk 1977; Pratt and McIntyre 1996) and it is used as an initial guide to fit the Fe^{3+} surface contribution to the Fe($2p_{3/2}$) spectrum (Figs. 3a and 3b).

Fe($2p_{3/2}$) peak assignments

Spectral contributions. Fe of bulk pyrite (Fig. 4) adopts a low-spin state (Fig. 4a) and it should contribute one peak (no multiplet splitting) to the Fe($2p_{3/2}$) spectrum. Surface Fe^{2+} and Fe^{3+} have unpaired electrons in the valence band (Figs. 4d and 4e) and both should exhibit a multiplet peak structure in the spectrum. The three likely contributions to the Fe($2p_{3/2}$) spectrum are a bulk Fe^{2+} singlet peak, a multiplet (triplet) contribution from surface Fe^{2+} ions and a multiplet (four peak) contribution from surface Fe^{3+} ions. Bulk Fe^{2+} is bonded only to disulfide, whereas the Fe^{2+} surface state may be bonded to both disulfide and monosulfide (S^{2-}).

Bulk Fe^{2+} contributions. The attenuation length of Fe photoelectrons is sufficiently great that bulk Fe^{2+} is the major contributor to the Fe($2p_{3/2}$) spectrum of Figure 3 (Tanuma et al. 1991). Bulk Fe^{2+} is in low-spin state (Fig. 4b). It is consequently represented by only one peak at 707.0 ± 0.1 eV, as observed in other studies (Nesbitt and Muir 1994; Mycroft et al. 1990; Buckley and Woods 1987).

Surface Fe^{3+} contributions. Fe^{3+} and Fe^{2+} are present in both magnetite (McIntyre and Zetaruk 1977) and pyrrhotite (Fe_7S_8, Pratt et al. 1994). The energy separating the Fe^{3+} multiplet peak of lowest binding energy from the Fe^{2+} main peak is about 1.75 eV in both minerals. The main Fe^{2+} peak of pyrite is near 707 eV so that the lowest energy multiplet peak of surface Fe^{3+} should be at about 708.75. This coincides with the binding energy of the small, partially resolved peak in the Fe($2p_{3/2}$) XPS spectrum near 709 eV (Figs. 3a and 3b). The binding energies separating the four multiplet peaks were taken as 1.0 eV, which is consistent with Fe^{3+} multiplet splittings obtained for pyrrhotite (Pratt et al. 1994), magnetite (McIntyre and Zetaruk 1977) and as calculated for the Fe^{3+} free ion (Gupta and Sen 1975). Full-width at half-minimum (FWHM) values were set equal to that of the bulk Fe^{2+} peak (707.0 eV peak). The Fe^{3+} multiplet peaks consequently was constrained with respect to binding energies and with respect to FWHM. The only adjustable parameters were the intensities of the four Fe^{3+} multiplet peaks. These were adjusted to obtain the best fit to the high-energy tail (Fig. 3). The resulting fit virtually mimics the

TABLE 1. Fe($2p_{3/2}$) XPS spectral peak parameters

Contribution	Binding energy (eV)	FWHM (eV)	Atomic percent	State
Fe^{2+} Bulk	707.00	0.85	73.8	Bulk
Fe^{3+} M1*	708.75	0.85	4.59	Surface
Fe^{3+} M2	709.85	0.85	3.45	Surface
Fe^{3+} M3	710.85	0.85	1.81	Surface
Fe^{3+} M4	711.85	0.85	0.51	Surface
Fe^{2+} M1	707.10	0.85	3.94	Surface
Fe^{2+} M2	708.05	0.85	7.92	Surface
Fe^{2+} M3	709.00	0.85	3.97	Surface

* Multiplet peaks are designated M and numbered.

XPS data in the region between 708.75 and 712 eV (Fig. 3b). Peak parameters are listed in Table 1.

Surface Fe^{2+} contributions. The spectral contribution of the surface Fe^{2+} state should be located at somewhat higher binding energy than the bulk Fe^{2+} contribution according to the arguments of Bronold et al. (1994). Removal of a ligand during fracture reduces the electrostatic repulsion on the Fe d states. Bronold et al. (1994) argue convincingly that as a consequence surface Fe^{2+} ions should be more electron-withholding than bulk Fe^{2+} ions (an electric double layer centered on the Fe^{2+} ions is created in the near-surface.) This should decrease the kinetic energy of photoelectrons derived from surface Fe^{2+} ions and increase their binding energy to a value somewhat greater than that of bulk Fe^{2+} photoemissions.

As noted previously, the multiplet structure for surface Fe^{2+} ions has been taken to contain three peaks, each separated by about 1 eV. The multiplets are also constrained to the same FWHM as that of the bulk Fe^{2+} peak. Intensities of the three peaks were adjusted to fit the spectrum. This surface Fe^{2+} contribution, if centered at 708.1 eV, provides an excellent fit to the Fe($2p_{3/2}$) spectrum. Peak parameters are listed in Table 1. Inclusion of the three contributions, bulk Fe^{2+} ions, surface Fe^{2+} ions, and surface Fe^{3+} ions provides an excellent fit to the Fe($2p_{3/2}$) XPS spectrum and the interpretation is adopted as the most reasonable considering the available evidence.

DISCUSSION

Likely surface sulfur species

Most previous interpretations of the S(2p) spectrum considered only disulfide ions to populate the pyrite fracture surface. We have considered a more realistic surface where rupture of S-S bonds has occurred and resulted in production of S^{2-} (monosulfide) and S_2^{2-} (surface disulfide), and possibly in formation of S_n^{2-} (polysulfide) and S^0 (elemental sulfur) surface species. Although the surface considered here is much more complicated than any considered previously, there may be additional contributions. The vagaries of S-S bond scission may lead to monosulfide (S^{2-}) bonded to one, two, or three Fe ions. Each S^{2-} of different coordination number may have a unique (but perhaps unresolved) contribution to the S(2p) spectrum near 161.3 eV. The broad nature of the peak at 161.3 eV (Fig. 2c) may reflect these contributions. The surface species giving rise to the peak remains, however, S^{2-}. Similarly, The surface-most S atom of surface disulfide ions may be bonded to zero, one, or two Fe ions, thus there may be three unique spectral contributions from this surface species. The number of S atoms in surface polysulfides may vary, each yielding a unique but unresolved spectral peak. Although there may be additional contributions to the S(2p) spectrum, the three considered here (Fig. 2c) are justified on the basis of the available evidence, and are sufficient to explain the major features of the S(2p) spectrum.

Proportion of S-S bonds broken

About equal numbers of disulfide and Fe ions should be exposed on a fracture surface. According to the interpretation of the Fe($2p_{3/2}$) spectrum, surface Fe ions constitute about 25% and bulk Fe about 75% of the Fe signal (Table 1). Of the Fe surface states almost 40% is Fe^{3+}, the remainder being Fe^{2+} (Table 1). For each S-S bond severed, there is production of one Fe^{3+} and one S^{2-} ion according to reaction 1. Because there should be about equal numbers of Fe and S atoms exposed on a fracture surface, these relations indicate that almost 40% of disulfide bonds exposed during fracturing are ruptured. Sixty percent of the surface disulfide remain intact. The surface-most disulfide of the dimer (Fig. 2b, state ''b'') and the monosulfide surface state (Fig. 2b, state ''a'') should display a ratio near 40/60. The peak heights of the two surface states (Fig. 2c, peaks at 162.0 and 161.3 eV) are close to this ratio.

Annealed and fractured surfaces

Chaturvedi et al. (1995) studied a He^+-bombarded and annealed pyrite surface and concluded that there was no monosulfide (S^{2-}) surface state. Bronold et al. (1994), Nesbitt and Muir (1994), and Pratt et al. (1998) observed a low-binding energy peak in S(2p) spectra of untreated, fractured pyrite surfaces. Mycroft et al. (1995) observe the same peak on polished pyrite surfaces. If the peak is absent from the bombarded and annealed surface, it clearly has different surface states from the fractured surface. This is possible considering the laboratory treatment of their surface. As emphasized by Gibson and LaFemina (1996), some surface states normally cannot be readily accessed due to kinetic inhibition. Ion etching and annealing pyrite surfaces may well provide the energy required to access additional, more stable states and a new configuration may have been achieved at the annealed pyrite surface. Annealing may, for example, allow monosulfide of fractured surfaces to migrate across the surface and react to produce disulfide species.

The absence of a surface state in the S(2p) spectrum of Chaturvedi et al. (1995) is nevertheless unexpected because the disulfide surface state at 162.0 eV (Fig. 2c) should have been observed. The fact that there is no indication of this peak in their spectrum strongly suggests that their resolution (FWHM of 1.3) is insufficient to

identify low-intensity surface states. Because the S^{2-} surface state at 161.3 eV is of lower intensity than the S_2^{2-} surface state (Fig. 2c, 162.0 eV), it is unlikely that the 161.3 surface state would be resolved in their spectrum. The aspect they address is, however, important to the understanding of surface properties of pyrite. Unfortunately, proof for the absence of a 161.3 eV peak on annealed surfaces awaits high-resolution studies (FWHM of peaks less than 0.9 eV). Experiments of the type conducted by Bronold et al. (1994) are particularly valuable.

Band gap, valence band edge, and reactivity

Eggleston et al. (1996) offered an elegant explanation for pyrite oxidation kinetics, but recent considerations of electronic states (Bronold et al. 1994) and our findings may require a somewhat more exhaustive treatment. The additional surface states may affect initiation of surface oxidation and may enhance or impede initial reaction rates. Importantly, Bronold et al. (1994) demonstrated that although the bulk band gap is 0.9 eV, the valence band edge is very close to the Fermi level due to the lowered symmetry imposed on surface species by fracturing the mineral. The valence band edge approaches closely the lower edge of the hematite conduction band (Eggleston et al. 1996) so that surface Fe species of pyrite may be more reactive than previously considered. Specifically, incorporation of calculations by Bronold et al. (1994) into the arguments of Eggleston et al. (1996), and consideration of the effects of S^{2-} Fe^{2+} and Fe^{3+} surface states, may result in surface Fe^{2+} of pyrite being a better reductant than heretofore appreciated. Rate constants for electron transfer may have to be modified to account for the two Fe surface states, the effects of S^{2-} on nearest-neighbor Fe ions, and to account for the effects of symmetry reduction (Bronold et al. 1994). We encourage and await additional developments that incorporate these results and the findings of Bronold et al. (1994) into the approach and framework developed by Eggleston et al. (1996).

Conclusions

The interpretation of the S(2p) and Fe(2p) spectra, although based on available evidence, is nevertheless speculative and needs to be tested. Bond strengths of Fe-S_2 must be evaluated in some detail, with both ionic and covalent considerations included. There is need for theoretical and mathematical studies focused on the multiplet peak structures of Fe(2p) signals (intermediate spin states especially). The methodology already has been established by Gupta and Sen (1974, 1975). Of vital importance is determination of coordination numbers of surface species and of lengths of bonds associated with the surface species. X-ray absorption spectroscopic studies (XANES and EXAFS) should be useful in this regard. Finally, the relative reactivities of the surface species are required to understand reaction mechanisms and rates during the initial stages of oxidation of the mineral. Synchrotron studies with appropriately tuned primary beam energies are underway.

Acknowledgments

We thank M. Fleet for discussions, D. Legrand and A. Schaufuss for insightful discussions and carefully reading the original manuscript, and G. Waychunas and two reviewers for their careful reviews and editorial suggestions, all of which improved the manuscript. This research was supported by grants to the first two authors from the National Science and Engineering Research Council of Canada.

References cited

Bronold, M., Tomm, Y., and Jaigermann, W. (1994) Surface states of cubic d-band semiconductor pyrite (FeS_2). Surface Science Letters, 314, L931–L936.

Buckley, A.N. and Woods, R. (1985) X-ray photoelectron spectroscopy of oxidized pyrrhotite surfaces II: Exposure to aqueous solutions. Applied Surface Science, 20, 472–480.

———(1987) The surface oxidation of pyrite. Applied Surface Science, 27, 437–452.

Buckley, A.N., Wouterlood, H.J, Cartwright, P.S., and Gillard, R.D. (1988) Core electron binding energies of platinum and rhodium polysulfides. Inorganica Chimica Acta, 143, 77–80.

Chaturvedi, S., Katz, R., Guevremont, J., Schoonen, M.A.A., and Strongin, D.R. (1996) XPS and LEED study of a single-crystal surface of pyrite. American Mineralogist, 81, 261–264.

Deer, W.A., Howie, R.A., and Zussman, J. (1992) An Introduction to the Rock-Forming Minerals, 696 p. (2nd ed.), Longmans, London.

Doniach, S. and Sunjic, M. (1970) Many-electron singularity in X-ray photoemission and X-ray line spectra of metals. Journal of Physics, C3, 285–291.

Eggleston, C.M., Ehrhardt, J.J., and Stumm, W. (1996) Surface structural controls on pyrite oxidation kinetics: An XPS-UPS, STM, and modeling study. American Mineralogist, 81, 1036–1056.

Gibson, A.S. and LaFemina, J.P. (1996) Structure of mineral surfaces. In P.V. Brady, Ed., Physics and Chemistry of Mineral Surfaces, 368 p. CRC Press, Boca Raton, Florida.

Goodenough, J.B. (1982) Iron sulfides. Annales de Chimie (France), 1, 489–503.

Gupta, R.P. and Sen, S.K. (1974) Calculation of multiplet structure of core p-vacancy levels. Physical Reviews, B10, 71–79.

———(1975) Calculation of multiplet structure of core p-vacancy levels II. Physical Reviews, B12, 12–19.

Harrison, W.A. (1980) Electronic Structure and the Properties of Solids, 582 p. Freeman, San Francisco, California.

Henrich, V.E. and Cox, P.A. (1994) The Surface Science of Metal Oxides, 464 p. Cambridge University Press. Cambridge, U.K.

Hyland, M.M. and Bancroft, G.M. (1989) An XPS study of gold deposition at low temperatures on sulfide minerals: reducing agents. Geochimica Cosmochimica Acta, 53, 367–372.

Huheey, J.E. (1978) Inorganic Chemistry, 889 p. (2nd ed.) Harper and Row, New York.

Johnson, D.A. (1982) Some Thermodynamic Aspects of Inorganic Chemistry, 282 p. (2nd ed.) Cambridge University Press, Cambridge, U.K.

Langmuir, D. (1997) Aqueous Environmental Geochemistry, 600 p. Prentice-Hall, Upper Saddle River, New Jersey.

Laajalehto, K., Kartio, I., Kaurila, T., Laiho, T., and Suoninen, E. (1996) Investigation of copper sulfide surfaces using synchrotron radiation excited photoemission spectroscopy. In H.J. Mathieu, B. Reihl, and E. Briggs, Eds., European Conference on Applications of Surface and Interface Analysis ECASIA'95. Wiley, New York, 717–720.

Legrand, D.L., Bancroft, G.M., and Nesbitt, H.W. (1998) Surface characterization of pentlandite ($Fe,Ni)_9S_8$, by X-ray photoelectron spectroscopy. International Journal of Mineral Processing, 51, 217–228.

McIntyre, N.S. and Zetaruk, D.G. (1977) X-ray photoelectron spectroscopic studies of iron oxides. Analytical Chemistry, 49, 1521–1529.

Mycroft, J.R., Nesbitt, H.W., and Pratt, A.R. (1995) X-ray photoelectron and auger electron spectroscopy of air-oxidized pyrrhotite: Distribution

of oxidized species with depth. Geochimica Cosmochimica Acta, 59, 721–733.

Mycroft, J.R., Bancroft, G.M., McIntyre, N.S., Lorimer, J.W., and Hill, I.R. (1990) Detection of sulfur and polysulfides on electrochemically oxidized pyrite surfaces by X-ray photoelectron spectroscopy and Raman spectroscopy. Journal of Electroanalytical Chemistry, 292, 139–152.

Nesbitt, H.W. and Muir, I.J. (1994) X-ray photoelectron spectroscopic study of a pristine pyrite surface reacted with water vapour and air. Geochimica Cosmochimica Acta, 58, 4667–4679.

Nesbitt, H.W., Muir, I.J., and Pratt, A.R. (1995) Oxidation of arsenopyrite by air and air-saturated, distilled water, and implications for mechanism of oxidation. Geochimica Cosmochimica Acta, 59, 1773–1786.

Pratt, A.R., McIntyre, N.S., and Splinter, S.J. (1998) Deconvolution of pyrite, marcasite and arsenopyrite XPS spectra using the maximum entropy method. Surface Science (in press).

Pratt, A.R. and McIntyre, N.S. (1996) Comment on ''Curve fitting of Cr 2p photoelectron spectra of Cr_2O_3 and CrF_3''. Surface and Interfacial Analysis, 24, 529–530.

Pratt, A.R., Muir, I.J., and Nesbitt, H.W. (1994) X-ray photoelectron and auger electron spectroscopic studies of pyrrhotite, and mechanism of air oxidation. Geochimica Cosmochimica Acta, 58, 827–841.

Tanuma, S., Powell, C.J., and Penn, D.R. (1991) Calculations of electron inelastic mean free paths III. SIA, Surface and Interfacial Analyses 17, 927–939.

Termes, S.C., Buckley, A.N., and Gillard, R.D. (1987) 2p electron binding energies for sulfur atoms in metal polysulfides. Inorganica Chimica Acta, 126, 79–82.

Manuscript received October 1, 1997
Manuscript accepted March 27, 1997
Paper handled by Glenn A. Waychunas